Oxid Met (2017) 87:801–811
DOI 10.1007/s11085-017-9763-z

ORIGINAL PAPER

Microstructural Study of the Influence of KCl and HCl on Preformed Corrosion Product Layers on Stainless Steel

M. A. Olivas-Ogaz[1] · J. Eklund[1] · J.-E. Svensson[1] · J. Liske[1] · T. Jonsson[1]

Received: 13 January 2017 / Published online: 4 March 2017

Abstract Metallic construction materials in biomass- and waste-fired boilers are exposed to corrosive environments due to the considerable amounts of alkali chlorides and HCl(g) released in renewable fuels combustion. Alkali chlorides corrosivity toward stainless steels exposed at high temperature has been extensively studied. Nevertheless, the corrosion attack propagation is still not fully understood and it is expected that chlorine diffusivity through oxide layers plays a major role in accelerating the corrosion. In order to investigate the role of chlorine on the propagation step of the corrosion attack, tailor-made oxides were produced. The samples were subsequently exposed to chlorine-containing environments for short period of time. The reaction atmospheres were $O_2 + H_2O + KCl(s)$ and $O_2 + H_2O + HCl(g)$ at 600 °C. Since in this study chlorine diffusivity through the corrosion product layer is of great interest, samples were analyzed with XRD and SEM/EDX. High-quality BIB cross sections were performed. Summarizing, for the preformed oxide layers on the stainless steel in the presence of HCl(g), chlorine

✉ M. A. Olivas-Ogaz
andrea.olivas@chalmers.se

J. Eklund
johekl@chalmers.se

J.-E. Svensson
jesper.liske@chalmers.se

J. Liske
jes@chalmers.se

T. Jonsson
torbjorn.jonsson@chalmers.se

[1] Department of Chemistry and Chemical Engineering, Environmental Inorganic Chemistry, High Temperature Corrosion Center, Chalmers University of Technology, 41296 Gothenburg, Sweden

seemed to penetrate to the oxide/metal interfaces in the material. However, in the presence of KCl(s) there seems to be no effect of the salt on the corrosion rate.

Keywords Cl-induced · Pre-oxidation · Chlorine · Scale

Introduction

The metallic construction materials (e.g., water walls and superheaters) of biomass- and waste-fired boilers are exposed to a more corrosive environment than corresponding fossil fuel-fired boilers. This is due to the presence of considerable amounts of alkali chlorides and HCl(g) in the flue gas originated from the combustion of biomass and waste fuels [1]. Depending on material temperature and position in the boiler, both low alloyed and stainless steels are being used in this kind of chlorine-rich environment. The stainless steels are usually used where the corrosive environment is most severe. Stainless steels rely on the formation of a dense corundum-type Cr-rich scale as protection toward the corrosive environment. However, in this type of environment these steels usually suffer from breakaway corrosion. After the breakaway of the protective Cr-rich oxide, the propagation of the corrosion attack will depend on the formation of a less protective Fe-rich oxide. The corrosivity of chlorine-rich environments at high temperature has been investigated earlier [2–14]. One of the corrosion mechanisms proposed for the onset of the corrosion attack is the "chromate formation" mechanism [3]. In this mechanism, the alkali chlorides, or alkali carbonate [15], react with the chromium in the protective oxide scale which leads to a Cr-depleted oxide and thereby breakaway corrosion. Other mechanism proposed for the accelerated corrosion attack in the presence of chlorine-rich environments is the "active oxidation" [5]. In this mechanism, the corrosion attack is proposed to be driven by the penetration of Cl_2 through the oxide scale toward the metal leading to the formation of metal chlorides at the oxide/metal interface. These metal chlorides have high vapor pressures and diffuse outwards to the gas/oxide interface. As the metal chlorides diffuse outward, they react with O_2 to form metal oxide and Cl_2. Another mechanism proposed for the accelerated corrosion in chlorine-rich environments is based on an electrochemical process involving chloride ions [16]. In this mechanism, the corrosion attack is suggested to start with the dissociation of HCl or Cl_2 into Cl^- at the oxide surface. The Cl^- ions diffuse along the grain boundaries of the oxide, forming metal chlorides [16]; in the case of pure iron, $FeCl_2$ forms throughout the oxide and at the gas/oxide interface [16, 17].

It still unclear how the chlorine is able to penetrate the scale (as gas Cl_2 or as Cl^- ions) and exactly how the presence of metal chlorides accelerates the corrosion attack. The present study is focused on the role of chlorine in the propagation step of the corrosion attack. The investigation was performed on stainless steel in oxidizing atmosphere at 600 °C. In order to follow the penetration of chlorine through the scale, tailor-made oxides were produced on the samples by pre-oxidation in different environments prior to the exposure containing KCl or HCl.

Experimental Procedures

Sample Preparation

The material used for this study was the stainless steel 347H, and Table 1 shows the chemical composition of the alloy. Plates of the alloy were cut into coupons with the dimensions of 15 mm × 15 mm with a thickness of 2 mm. In order to simplify the sample handling, a hole of 1.5 mm diameter was drilled. The coupons were ground down to 320 grit on SiC paper and polished down to 1 μm diamond suspension until mirror like surface. After polishing, the samples were cleaned and degreased with acetone and ethanol in ultrasonic agitation bath.

Prior exposure to the chlorine-containing environment, the samples were pre-oxidized. The pre-oxidation atmosphere consisted of $5\%O_2 + 95\%N_2$, and the samples were sprayed with 1.35 μmol K^+/cm^2 in form of K_2CO_3 prior to the pre-oxidation. The presence of K_2CO_3 is used to accelerate the breakaway of the protective oxide layer characteristic of stainless steels, and Fe-rich oxide is aimed with this pre-oxidation. The pre-oxidation temperature was set at 600 °C, and the time was 168 h.

After pre-oxidation, the samples were exposed either to HCl(g) or KCl(s). The aim of selecting HCl(g) and KCl(s), based on earlier studies [16, 18, 19], as corrosive species after pre-oxidation is to investigate any difference in the propagation attack, e.g., diffusion of chlorine through the oxide scale. In the presence of HCl(g), the atmosphere consisted of $5\%O_2 + 20\%H_2O + 500$ ppm $HCl + N_2$, and the HCl was added from a $1\%HCl–99\%N_2$ pre-mixed gas using digital mass flow controller. In the presence of KCl(s), the reaction atmosphere was $5\%O_2 + 20\%H_2O + N_2$, and the salt was deposited prior to exposure on the samples surface by spraying a saturated solution in a 20:80 volume ratio water–ethanol mixture and dried with warm air; the amount of salt deposited on each sample was about 0.10 mg/cm^2 (corresponding to 1.35 μmol K^+/cm^2). Pre-oxidized samples in the absence of chlorine were also exposed and used as references. All samples were stored in desiccators before and after exposure to prevent atmospheric corrosion.

The exposures were performed isothermally in horizontal silica tube furnaces. The temperature was maintained at 600 ± 1 °C. The exposure time was 24 h. The flow rate was of 2.5 cm/s and calibrated by a Bios Definer 220M. In order to prevent any condensation of water in the system, all parts were kept over 100 °C. The samples were placed in the center of the furnace, mounted vertically on an alumina sample holder with a capacity of three samples. The weight of the samples was measured before and after the exposure using a Sartorius™ balance with microgram resolution.

Table 1 Chemical composition of the alloy

Alloy	Fe	Cr	Ni	Mn	Si	C
347H	Bal	17.6	10.1	1.6	0.6	0.05

Cross sections of the corroded samples were prepared by dry cutting with a low-speed diamond saw and subsequent broad ion beam (BIB) milling with a Leica TIC 3X instrument. The device is equipped with three argon ion guns for sputtering. The guns were operated at 6 kV, and the total sputtering time was 6 h. The site of interest was positioned with an optical microscope. Prior to milling, the sample was sputter-coated with gold and a thin polished silicon wafer was applied on the surface in order to protect the oxide scale during cutting and to render a smooth cross section after milling.

The samples were analyzed by means of scanning electron microscopy (SEM) and energy-dispersive X-ray spectroscopy (EDX) using an FEI Quanta 200 equipped with an Oxford Instruments X-Max^N 80 T EDX detector and a Zeiss Ultra 55 scanning electron microscope (SEM). For XRD analysis, a Siemens D5000 powder diffractometer with grazing-incidence geometry was used. The thermodynamic calculations were performed using the software FactSage 7.0 and database: FactPS 7.0.

Results and Discussion

Pre-oxidation

In order to study the role of chlorine [both as KCl(s) and as HCl(g)] in the propagation step, 347H was pre-oxidized to form an oxide scale indicative for a stainless steel which has gone into breakaway oxidation. This was achieved by exposing 347H at 600 °C for 168 h in 5%O_2 + N_2 + K_2CO_3(s). The pre-oxidation parameters were selected based on earlier work [6, 15, 20] to achieve Fe-rich oxide. The mechanism for breakaway oxidation in the presence of K_2CO_3 has previously been proposed to be caused by chromate formation on the sample surface [15]. The stability of the potassium chromate formed on corroding stainless steel samples has earlier been reported to be low, and after 168 h, it is seldom detected [6, 21, 22]. Thus, the chromate formation is primarily important in the initiation of the corrosion.

In Fig. 1, a cross-sectional view of the pre-oxidized sample is shown. The corrosion morphology is characterized by a two-layered oxide with a total thickness of approximately 6 μm which was the aim when selecting the pre-oxidation parameters. According to the SEM/EDX and XRD, the outward growing layer is suggested to be hematite (Fe_2O_3). The inward growing part is showing the characteristics of a spinel oxide containing iron, chromium and nickel. As can be seen, the inward growing oxide is not homogenous and a layered structure is seen, see Fig. 1. This type of morphology is expected to be the result of the fully oxidized regions of previously formed reaction zones [20]. Some pores are observed at the lower part of the Fe_2O_3, i.e., the former metal surface, as well as the metal/oxide interface. On the pre-oxidized 347H sample, a correlation between potassium and iron was found, and according to XRD analysis, $KFeO_2$ was detected. Furthermore, at the metal/oxide interface, a nickel enrichment was detected in the metal.

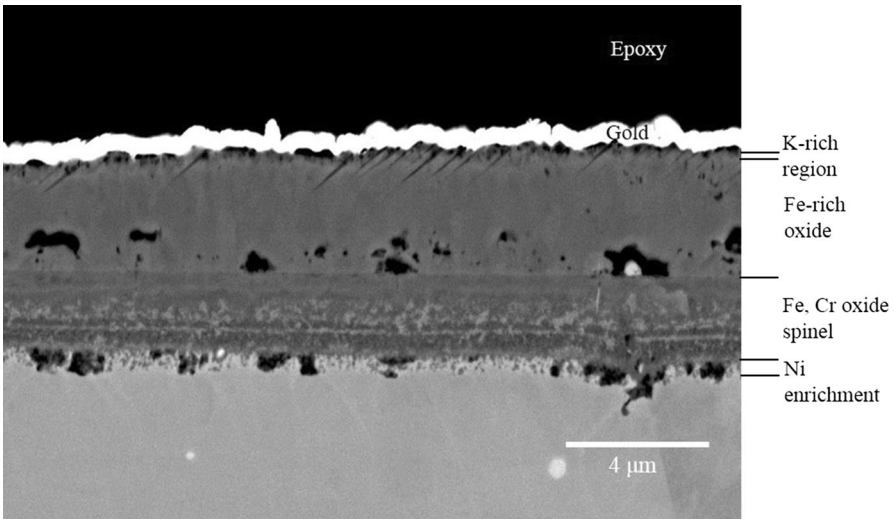

Fig. 1 BSE image of cross section of pre-oxidized 347H at 600 °C for 168 h in $5\%O_2 + N_2 + 1.35$ µmol K^+/cm^2 using K_2CO_3

Scale Microstructure After Exposure to KCl(s)

After being pre-oxidized, the 347H samples were exposed to chlorine either in the form of KCl(s) or HCl(g). SEM images of both plan view and cross sections of the exposed samples are shown in Fig. 2. The samples exposed to KCl(s) are shown in Fig. 2a (plan view SEM) and Fig. 2c (cross-sectional SEM), respectively. The sample surface reveals a surface being covered by various sized oxides. The rough oxide nodules are suggested to be the location of former KCl particles which has been overgrown by oxides. In general, no cracks were seen in the plan view image. In the cross-sectional view (Fig. 2c), the corrosion product layer is measured to be roughly 7–9 µm. The corrosion morphology is similar as after the pre-oxidation, showing the presence of inward growing/outward growing oxide scales and the presence of some voids.

EDX analysis has been performed at the cross section shown in Fig. 2c, see Fig. 3. According to the analysis, the composition of the two oxide layers is similar to the oxide layers formed after pre-oxidation with K_2CO_3. The outward growing oxide layer is mainly composed of iron which complies well with the presence of Fe_2O_3 detected by XRD. The inward growing oxide layer is composed of a mixed spinel. In addition, in the outermost part of the top layer potassium is detected, whereas the amount of chlorine is low. Since no signs of spallation were detected for the KCl-exposed samples, it is suggested that most of the KCl applied has evaporated during the exposure. However, potassium may be correlated to iron and according to the XRD analysis $KFeO_2$ was detected on the sample. The evaporation of KCl(s) applied ex situ to an already corroded surface and subsequently exposed in this type of experimental setup at 600 °C has been observed earlier by Karlsson [23].

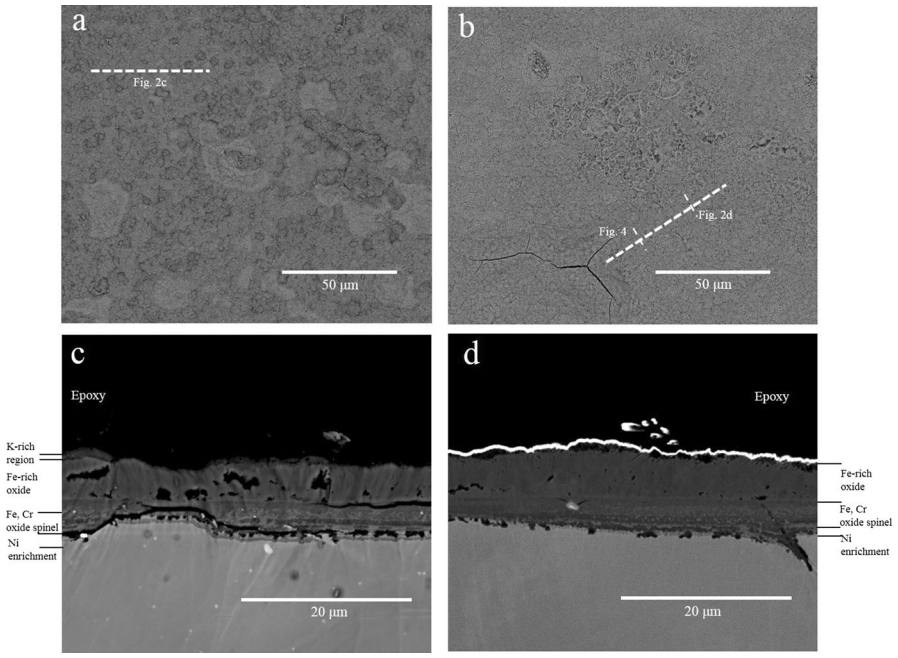

Fig. 2 BSE image of pre-oxidized 347H after exposure to 5%O_2 + 20%H_2O + N_2 for 24 h at 600 °C: **a** in the presence of KCl(s), *plan view*; **b** in the presence of HCl(g), *plan view*; **c** in the presence of KCl(g), *cross-sectional view*; **d** in the presence of HCl(g), *cross-sectional view*

Scale Microstructure After Exposure to HCl(g)

For the pre-oxidized sample being exposed in the presence of HCl(g), the morphology of the sample surface was slightly different compared to the KCl(s)-exposed samples, see Fig. 2a, b. Compared to the samples exposed to KCl(s), the surface is much more smooth and homogenous. However, cracks in the oxide layer can be seen. Cross-sectional SEM analysis was performed on areas composing the majority of the sample surface and on areas close to cracks (see Fig. 4). According to the SEM/EDX analysis of the area with well-adherent oxide layers, the composition and thickness are similar to the corresponding oxides formed in the presence of KCl(s) affecting the corrosion morphology very little. The oxide scales increased from about 6 µm after pre-oxidation to 7–9 µm after exposure to HCl(g). However, signs of steel grain boundary attack were seen in the presence of HCl(g). The growth rate of the corrosion product layers in the presence of either KCl(s) or HCl(g) after the initial pre-oxidation is not significantly higher compared to the expected growth rate in the absence of these chloride salts [15]. Hence, after the initial corrosion attack the presence of chlorine does not accelerate the attack, at least not during the first 24 h after applied to the corroded surface. However, the presence of HCl(g) seems to induce some cracks and spallation of the oxide, see Fig. 2b.

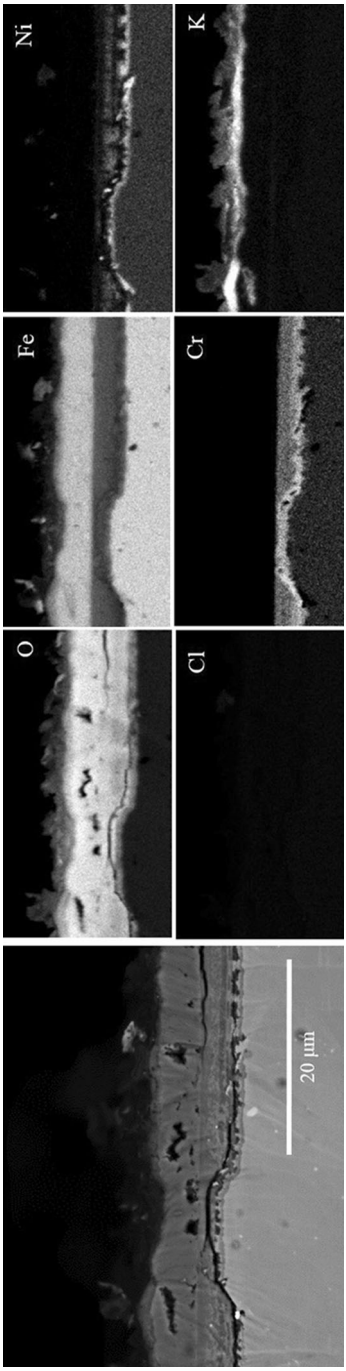

Fig. 3 EDX mapping of pre-oxidized 347H after exposure to $5\%O_2 + 20\%H_2O + N_2$ for 24 h in the presence of KCl(s)

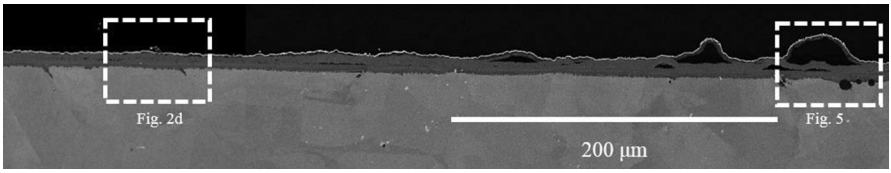

Fig. 4 BIB cross section of the pre-oxidized 347H after exposure to 5% O_2 + 20% H_2O + 500 ppm HCl + N_2 for 24 h

A large BIB cross section of the pre-oxidized samples exposed in the presence of 500 ppm HCl(g) is shown in Fig. 4. The plan view SEM analysis of the sample is shown in Fig. 2b, and it revealed two distinct features in the surface; a smooth oxide covering the majority of the sample surface together with areas where large cracks were seen. All samples exposed to HCl(g) suffered from spallation. From the BIB cross section shown in Fig. 4, it is rather clear that the spallation and cracking of the oxide are located to the areas where large blisters/voids could be seen. EDX analysis of this region is shown in Fig. 5. In contrast to the KCl-exposed sample, the potassium-rich layer on top of the sample surface seen after pre-oxidation with K_2CO_3 was no longer present. According to thermodynamical calculations, the $KFeO_2$ detected by XRD after pre-oxidation with K_2CO_3 is suggested to react with the HCl(g) to form KCl(s). The equilibrium partial pressure of KCl(g) over KCl(s) at 600 °C is 3.4 ppm. Due to the experimental setup used, where the gas flow has been set at 2.5 cm/s, it might not be possible to detect any KCl(s) on the surface after 24 h, i.e., the KCl(s) might be lost as KCl(g). In earlier work by Pettersson et al. [15], the amount of KCl(s) remaining on 304L stainless steel sample after being sprayed ex situ with 0.10 mg/cm^2 KCl (corresponding to the same molar amount of potassium as for K_2CO_3) was less than 1% after 24 h at 600 °C. The same result was observed when 304L was pre-oxidized in the presence of KCl(s) and subsequently exposed in the presence of KCl(s); the amount of KCl remaining on the sample after the exposure was below detection [23]. The XRD results of the pre-oxidized 347H sample exposed in the presence of HCl showed no presence of any potassium containing phases.

The EDX analysis of the cracked region is shown in Fig. 5. The analysis reveals that the blister formation is occurring in the outward growing Fe_2O_3 layer. From the BIB cross section shown in Fig. 4, it can be seen that this is true throughout the scale, and the detachment is occurring primarily in the outward growing oxide layer and in the interface between the outward growing and inward growing oxide scales. Presence of chlorine was detected at the oxide/metal interface beneath a region with blisters. The presence of potassium was low in this point, and the chlorine is in the form of a metal chloride. According to the XRD results, weak signals of iron and chromium chlorides were detected. The cross-sectional SEM/EDX analysis did not detect any chlorine in the outer part of the oxide or in the blisters. Hence, it is not really clear how these large blisters have appeared and further studies are needed. Especially, high-resolution microscopy techniques, e.g., TEM, may be used in order to investigate these layers in closer detail. It may, however, be stressed that the amount of metal chlorides detected on sample was small and the overall corrosion

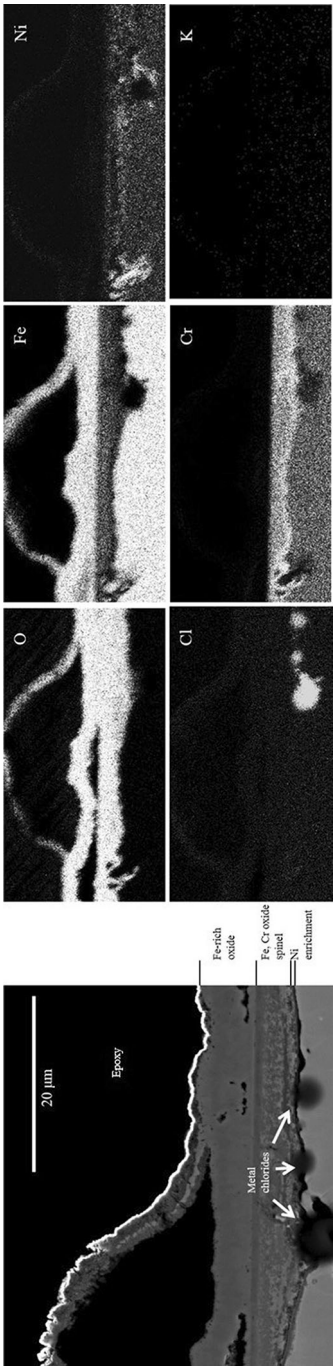

Fig. 5 EDX mapping of pre-oxidized 347H after exposure to 5% O_2 + 20% H_2O + 500 ppm HCl + N_2 for 24 h

attack was limited as well as being in the same range as for the KCl(s)-exposed sample.

Conclusions

In this study, the stainless steel 347H was pre-oxidized in the presence of K_2CO_3 and subsequently exposed to KCl(s) or HCl(g) at 600 °C. The aim of the study was to investigate the role of chlorine-containing species in the propagation stages after the initial corrosion attack, i.e., the stainless steel had already formed a corrosion product layer prior to the exposure. This was done by pre-oxidizing 347H in the presence of K_2CO_3 and thereby forming an outward-growing Fe_2O_3 layer and an inward growing spinel oxide. Furthermore, the pre-oxidation resulted in the formation of a $KFeO_2$ layer on the outermost surface.

- When the pre-oxidized 347H was exposed in the presence of 0.1 mg/cm^2 KCl(s) for 24 h at 600 °C, there was no or little tendency of accelerating the corrosion attack. Instead, the applied KCl(s) evaporates from the surface and there was no evidence of the salt interacting with the oxide or metal beneath, i.e., no metal chlorides were observed.
- When the pre-oxidized 347H was exposed in the presence of 500 ppm HCl(g) for 24 h at 600 °C, the majority of the sample surface was rather unaffected, following the same corrosion rate as for the KCl(s)-exposed samples. However, parts of the oxide scale show formation of iron oxide blisters and cracks leading to spallation and poor protection against this environment. Metal chlorides in the metal/oxide interface were also detected in this type of region where the presence of Fe_2O_3 blisters was found. Furthermore, the potassium ferrite present from the pre-oxidation step reacted with the HCl(g) to form Fe_2O_3 and KCl(s). The KCl formed evaporated, and after 24 h no or little potassium remained on the surface.

To conclude, the first 24 h of the propagation stage of the stainless steel 347H does not seem to be accelerated greatly by either KCl(s) or HCl(g). However, there are areas where the corrosion attack progressed in the presence of HCl(g) and longer exposure times may result in accelerated corrosion. Further studies with help of advanced microscopy focused on the role of oxide microstructure in the diffusion of chlorine species are needed.

Acknowledgements This work was carried out within the Swedish High Temperature Corrosion Centre (HTC) at Chalmers University of Technology.

References

1. H. P. Nielsen, F. J. Frandsen, K. Dam-Johansen, and L. L. Baxter, *Progress in Energy and Combustion Science* **26**, 283–298 (2000).
2. C. Pettersson, L. G. Johansson and J.-E. Svensson, *Materials Science Forum* **522–523**, 539–546 (2006).
3. J. Pettersson, H. Asteman, and J. E. Svensson, *Oxidation of Metals* **64**, 23–41 (2005).
4. J. Pettersson, J. E. Svensson and L. G. Johansson, *Materials Science Forum* **595–598**, 367–375 (2008).
5. H. J. Grabke, E. Reese and M. Spiegel, *Corrosion Science* **37**, 1023–1043 (1995).
6. J. Lehmusto, B. J. Skrifvars, P. Yrjas, and M. Hupa, *Fuel Processing Technology* **105**, 98–105 (2013).
7. S. Y. Lee, and M. J. McNallan, *Corrosion* **47**, 868–874 (1991).
8. S. Y. Lee, and M. J. McNallan, *Journal of the Electrochemical Society* **137**, 472–479 (1990).
9. Y. Shinata, *Oxidation of Metals* **27**, 315–332 (1987).
10. R. Bender, and M. Schutze, *Materials and Corrosion* **54**, 567–586 (2003).
11. V. A. C. Haanappel, N. W. J. Haanappel, T. Fransen, H. D. Van Corbach, and P. J. Gellings, *Corrosion* **48**, 812–821 (1992).
12. A. S. Kim, and M. J. McNallan, *Corrosion* **46**, 746–755 (1990).
13. X. J. Zheng, and R. A. Rapp, *Oxidation of Metals* **48**, 553–596 (1997).
14. S. Kiamehr, K. V. Dahl, M. Montgomery, and M. A. Somers, *Materials and Corrosion* **66**, 1414–1429 (2015).
15. J. Pettersson, N. Folkeson, L. G. Johansson, and J. Svensson, *Oxidation of Metals* **76**, 93–109 (2011).
16. N. Folkeson, L.-G. Johansson, and J.-E. Svensson, *Journal of The Electrochemical Society* **154**, C515–C521 (2007).
17. A. Zahs, M. Spiegel, and H. J. Grabke, *Materials and Corrosion-Werkstoffe Und Korrosion* **50**, 561–578 (1999).
18. S. Karlsson, J. Pettersson, L. G. Johansson, and J. E. Svensson, *Oxidation of Metals* **78**, 83–102 (2012).
19. C. Pettersson, J. Pettersson, H. Asteman, J. E. Svensson, and L. G. Johansson, *Corrosion Science* **48**, 1368–1378 (2006).
20. T. Jonsson, S. Karlsson, H. Hooshyar, M. Sattari, J. Liske, J. E. Svensson, and L. G. Johansson, *Oxidation of Metals* **85**, 509–536 (2016).
21. T. Jonsson, J. Froitzheim, J. Pettersson, J. E. Svensson, L. G. Johansson, and M. Halvarsson, *Oxidation of Metals* **72**, 213–239 (2009).
22. N. Israelsson, K. Hellström, J. E. Svensson, and L. G. Johansson, *Oxidation of Metals* **83**, 1–27 (2014).
23. S. Karlsson, *Reducing Alkali Chloride-Induced High Temperature Corrosion by Sulphur Containing Additives: A Combined Laboratory and Field Study* (Chalmers University of Technology, Göteborg, 2015).